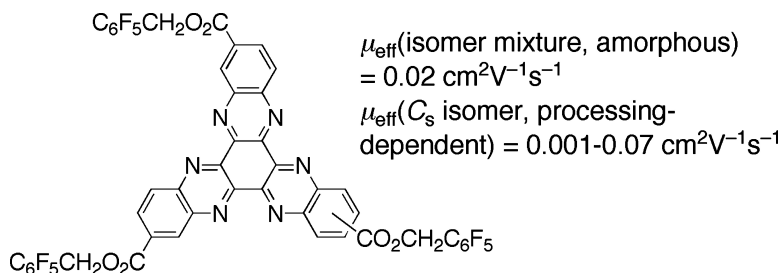


High Charge-Carrier Mobility in an Amorphous Hexaazatrinaphthylene Derivative

Bilal R. Kaafarani, Takeshi Kondo, Junsheng Yu, Qing Zhang, Davide Dattilo, Chad Risko, Simon C. Jones, Stephen Barlow, Benoit Domercq, Fabrice Amy, Antoine Kahn, Jean-Luc Brdas, Bernard Kippelen, and Seth R. Marder

J. Am. Chem. Soc., **2005**, 127 (47), 16358-16359 • DOI: 10.1021/ja0553147 • Publication Date (Web): 05 November 2005

Downloaded from <http://pubs.acs.org> on March 25, 2009



More About This Article

Additional resources and features associated with this article are available within the HTML version:

- Supporting Information
- Links to the 11 articles that cite this article, as of the time of this article download
- Access to high resolution figures
- Links to articles and content related to this article
- Copyright permission to reproduce figures and/or text from this article

[View the Full Text HTML](#)

High Charge-Carrier Mobility in an Amorphous Hexaazatrinaphthylene Derivative

Bilal R. Kaafarani,^{†,‡,¶} Takeshi Kondo,^{†,‡,§} Junsheng Yu,[§] Qing Zhang,[†] Davide Dattilo,[‡] Chad Risko,[†] Simon C. Jones,[†] Stephen Barlow,^{†,‡} Benoit Domercq,[§] Fabrice Amy,^{||} Antoine Kahn,^{||} Jean-Luc Brédas,[†] Bernard Kippelen,^{*,§} and Seth R. Marder^{*,†,‡}

Center for Organic Photonics and Electronics (COPE), School of Chemistry and Biochemistry, and School of Electrical and Computer Engineering, Georgia Institute of Technology, Atlanta, Georgia 30332, Department of Chemistry, University of Arizona, Tucson, Arizona 85721, and Department of Electrical Engineering, Princeton University, Princeton, New Jersey 08544

Received August 4, 2005; E-mail: seth.marder@chemistry.gatech.edu

New electron-transport (ET) organic materials that can readily be processed from solution are required for organic electronics and optoelectronics. The 5,6,11,12,17,18-hexaazatrinaphthylene (HATNA) ring has recently been identified as a potential component of ET materials, due to its ease of reduction and its ability, when suitably substituted, to self-assemble into columnar structures with large bandwidths.^{1,2} Recently, mobilities as high as $0.9 \text{ cm}^2 \text{ V}^{-1} \text{ s}^{-1}$ have been measured using the pulse-radiolysis time-resolved microwave conductivity technique in the crystalline phases of hexa-(alkylsulfanyl) derivatives.³ Here we report on a new tris(pentafluorobenzyl ester) derivative, **3** (Figure 1); both morphology and the effective charge-carrier mobility of thin films depend on whether pure **3b** or a **3a/b** isomer mixture is used, but we have measured effective mobilities as high as $0.07 \text{ cm}^2 \text{ V}^{-1} \text{ s}^{-1}$.

Bock and co-workers have previously reported the condensation of hexaketocyclohexane with 3,4-diaminobenzoic acid and esterification of the resulting tri(carboxylic acid) (Figure 1, $Z = \text{CO}_2\text{H}$) with a range of alcohols.¹ They report that these ester species are formed solely as the less symmetrical (C_s) 2,8,15- (**b**) isomer (Figure 1). In contrast, we obtain **3** (and, therefore, presumably also the poorly soluble triacid precursor) as an approximately statistical (1:3) mixture of the **a** (C_{3h}) and **b** isomers; these isomers can be distinguished by HPLC (two fractions with indistinguishable UV-vis spectra) and can be isolated in large quantities using recrystallization from CH_2Cl_2 (**3a**, isomer purity >92%) or column chromatography (**3b**, >90%). The NMR chemical shifts and line widths and, therefore, the apparent numbers and multiplicities of peaks are strongly dependent on concentration, presumably due to aggregation effects. However, the isomers can clearly be distinguished by high-field ^1H or ^{19}F NMR studies at moderate concentrations (ca. 10^{-3} M ; see Supporting Information).

We have determined the ionization potential (IP) of a film of the parent HATNA, **1**⁴ (vapor deposited on Au), to be $6.6 \pm 0.1 \text{ eV}$ using photoelectron spectroscopy (PES) and the electron affinity (EA) to be $-2.8 \pm 0.4 \text{ eV}$ using inverse photoelectron spectroscopy (IPES). One can, therefore, anticipate that the electron-withdrawing ester groups of **2** and **3** will lead to EAs $< -2.8 \text{ eV}$ and IPs $> 6.6 \text{ eV}$, if one assumes that solid-state aggregation has similar effects on EA and IP for each compound. Indeed, DFT calculations show gas-phase adiabatic EAs of -1.40 , -1.89 , and -2.09 eV for **1**, **2** ($R = \text{Me}$), and **3**, respectively, and IPs of 7.56 , 7.72 , and 7.78 eV .

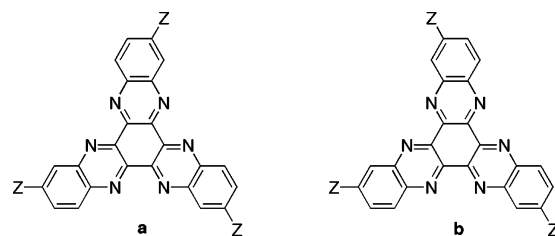


Figure 1. Structure of HATNAs. For compound **1**, $Z = \text{H}$; for **2**, $Z = \text{CO}_2\text{R}$ [$R = \text{alkyl}$]; for **3**, $Z = \text{CO}_2\text{CH}_2\text{C}_6\text{F}_5$.

The calculations also indicate that the small difference in the EAs of **2** and **3** is due to inductive effects; in both cases, the LUMO is restricted to the core and, to a lesser extent, the ester substituents, with negligible coefficients on the R groups. Electrochemical measurements are potentially also complicated by the affects of aggregation; however, we observed reversible reductions for **1**, **2** ($R = \text{Et}$), and **3** at -1.44 , -1.17 , and -1.12 V , respectively (vs $\text{FcCp}_2^{+/0}$, ca. 10^{-4} M in $\text{CH}_2\text{Cl}_2/0.1 \text{ M}$ [$^n\text{Bu}_4\text{N}$]⁺[PF_6]⁻), consistent with the DFT EA trends for isolated molecules and suggesting a solid-state EA of ca. -3.1 eV for **3**.⁵

According to DFT calculations, the reorganization energy for the electron-exchange reaction between **3** and **3**⁻ (0.20 eV) is larger than that for the parent **1/1**⁻ system (0.10 eV); however, it is still lower than the value estimated in the same way for $\text{Alq}_3/\text{Alq}_3^-$ (0.28 eV ⁶) or for TPD^+/TPD (0.29 eV ⁷), suggesting a low barrier for ET in **3**.

Thin films of a **3a/b** isomer mixture (ca. 1:3) and of pure **3b** were obtained on cooling from above the isotropic melting point 290 and $295 \text{ }^\circ\text{C}$, respectively (as measured by DSC) between two ITO-coated glass slides with calibrated glass spacers. X-ray diffraction data were obtained on samples prepared in a similar way without the top slide. The absence of diffraction peaks in the X-ray pattern, together with the absence of a texture under polarized optical microscopy (POM), suggests that mixed-isomer films are amorphous; these films show no evidence of crystallization after storage at room temperature for 18 months. Films obtained by rapidly cooling ($100 \text{ }^\circ\text{C}/\text{min}$) **3b** show a distinct texture under POM and show weak X-ray diffraction patterns (Figure 2). In more slowly cooled ($< 15 \text{ }^\circ\text{C}/\text{min}$) samples of **3b**, spherulite textures with dimensions of several millimeters are observed using POM.

The effective charge-carrier mobility in films of **3** was studied by the steady-state space-charge limited current (SCLC) technique.⁸ Figure 3 shows the current-density/voltage (J - V) characteristics of a sample with structure ITO/**3b** ($5 \mu\text{m}$)/ITO under ambient conditions. We extracted effective mobility values, μ_{eff} , by fitting the nearly quadratic region of the J - V curve according to the

[†] COPE and School of Chemistry and Biochemistry, Georgia Tech.

[‡] University of Arizona.

[§] COPE and School of Electrical and Computer Engineering, Georgia Tech.

^{||} Princeton University.

^{*} Current address: Department of Chemistry, American University of Beirut, Beirut, Lebanon.

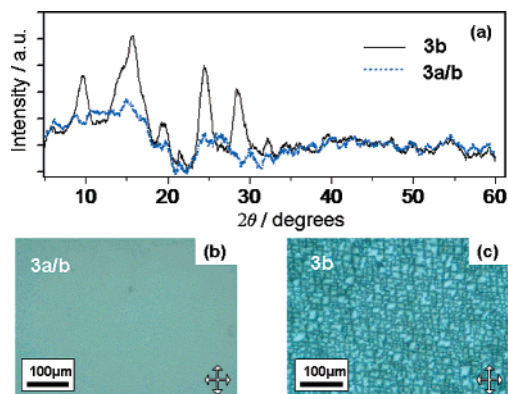


Figure 2. (a) X-ray diffraction at room temperature from rapidly cooled (100 °C/min) films of **3a/b** (ca. 1:3) on glass (background due to glass subtracted and data smoothed). Panels (b) and (c) are cross-polarized optical microscopy images of the same samples.

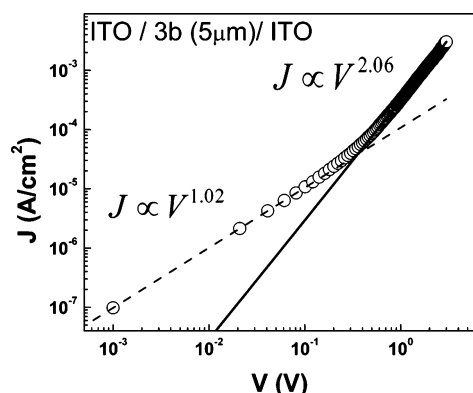


Figure 3. Typical current density, J , versus voltage, V , of an ITO/**3b** (5 μm)/ITO device in the dark and ambient conditions. The solid lines represent the predictions from a SCLC model including the field-dependent mobility of eq 1. The dashed line represents Ohm's law.

equation⁹

$$J = \frac{9}{8} \epsilon_0 \epsilon_r \mu_0 \exp\left(0.891 \gamma \sqrt{\frac{V}{d}}\right) \frac{V^2}{d^3} \quad (1)$$

where ϵ_0 is the permittivity of free space, ϵ_r is the relative dielectric constant of the active material estimated from capacitance measurements, d is the film thickness, μ_0 is the zero-field mobility, and γ is the field activation coefficient. Equation 1 is a modified version of the Mott–Gurney¹⁰ equation that takes into account the fact that the mobility in organics typically varies with electric field, E , according to

$$\mu_{\text{eff}} = \mu_0 \exp(\gamma \sqrt{E}) \quad (2)$$

Values of μ_{eff} at given electric fields were calculated according to eq 2 using values of μ_0 and γ obtained through the fitting procedure of the J – V characteristic in the quadratic (SCLC) region with eq 1. For the mixed-isomer film, we obtained a maximum effective mobility of 0.02 $\text{cm}^2 \text{V}^{-1} \text{s}^{-1}$. The effective mobility is one of the highest reported for an amorphous material.¹¹ In devices based on rapidly cooled pure **3b** (poorly crystalline), an even higher mobility of ca. 0.07 $\text{cm}^2 \text{V}^{-1} \text{s}^{-1}$ was measured (Figure 3), but a value of only 0.001 $\text{cm}^2 \text{V}^{-1} \text{s}^{-1}$ was obtained for a more slowly cooled

sample (exhibiting a spherulite texture on the millimeter length scale under POM), emphasizing the important influence of morphology on mobility. We have been unable to acquire mobility data for films of pure **3a** due to the strong tendency of these films to crystallize and to delaminate from the electrodes. Although, due to the different techniques employed, the mobilities for **3** cannot be directly compared to the high mobilities reported for HATNAs in ref 3, it is interesting to note that in both cases the highest mobilities were achieved in materials showing at least some crystallinity.

The estimated EA and IP values for **3** suggest that the barrier to electron injection into **3** from ITO ($E_{\text{Fermi}} \approx 4.5$ eV) is considerably lower than that for hole injection and, hence, that the majority of charge carriers in **3** are likely to be electrons, and therefore, our μ_{eff} values are likely to represent *electron* mobilities.

In conclusion, we have found that tris(ester) derivatives of HATNA are obtained as a statistical mixture of the two possible isomers, in contrast to a previous report that the pure 2,8,14-isomer is obtained. The presence of two isomers can have important implications for film morphology and effective mobility. In **3**, the statistical isomer mixture forms amorphous films with excellent temporal stability, which show an effective mobility that is the highest yet reported for an amorphous material. In contrast, films of the pure isomers, **3a** and **3b**, show tendencies to crystallize; **3b** films can exhibit widely differing morphologies and carrier mobilities depending critically on the processing conditions. These results suggest that these materials may be promising active components of electronic and optoelectronic devices, due to the potential to control morphologies and mobilities by changing the isomer ratio.

Acknowledgment. This material is based upon work supported in part by the STC Program of the NSF under agreement number DMR-0120967. We also thank Lintec Corporation, the NSF (CHE-0211419), and the ONR for support.

Supporting Information Available: Experimental and computational details, HPLC traces and ¹H and ¹⁹F NMR spectra of **3a**, **3b**, and mixtures, electrochemical data, PES, and IPES spectra of **1**, POM images of **3a** films and of slow-cooled **3b**, summary of mobility characteristics, and complete citation for refs 2c, 2d, and 3. This material is available free of charge via the Internet at <http://pubs.acs.org>.

References

- (1) Bock, H.; Babeau, A.; Seguy, I.; Jolinet, P.; Destruel, P. *ChemPhysChem* **2002**, *3*, 532.
- (2) (a) Ong, C. W.; Liao, S.-C.; Chang, T. H.; Hsu, H.-F. *Tetrahedron Lett.* **2003**, *44*, 1477. (b) Ong, C. W.; Liao, S.-C.; Chang, T. H.; Hsu, H.-F. *J. Org. Chem.* **2004**, *69*, 3181. (c) Crispin, X. et al. *J. Am. Chem. Soc.* **2004**, *126*, 11889. (d) Lemaire, V. et al. *J. Am. Chem. Soc.* **2004**, *126*, 3271.
- (3) Lehmann, M. et al. *Chem.–Eur. J.* **2005**, *11*, 3349.
- (4) Skujins, S.; Webb, G. A. *Tetrahedron* **1969**, *25*, 3935.
- (5) Bock (ref 1) has previously estimated IP and EA values of 6.3 and –3.4 eV, respectively, for alkyl esters (**2**) based on $E_{1/2}(\text{ester}^{+/0})$ (we were unable to observe this process in CH_2Cl_2), the IP of ferrocene, and optical data.
- (6) Lin, B. C.; Cheng, C. P.; You, Z.-Q.; Hsu, C.-P. *J. Am. Chem. Soc.* **2005**, *127*, 66.
- (7) Malagoli, M.; Brédas, J. L. *Chem. Phys. Lett.* **2000**, *327*, 13.
- (8) (a) Rose, A. *Phys. Rev.* **1955**, *97*, 1538. (b) Blom, P. W. M.; de Jong, M. J. M.; van Munster, M. G. *Phys. Rev. B* **1997**, *55*, R656. (c) Mihailetchi, V. D.; van Duren, K. J.; Blom, P. W. M.; Hummelen, J. C.; Janssen, R. A. J.; Kroon, J. M.; Rispen, M. T.; Verhees, W. J. H.; Wienk, M. M. *Adv. Funct. Mater.* **2003**, *13*, 43.
- (9) Murgatroyd, P. N. *J. Phys.* **1970**, *D3*, 151.
- (10) (a) Mott, N. F.; Gurney, D. *Electronic Processes in Ionic Crystals*; Academic Press: New York, 1970. (b) Campbell, A. J.; Bradley, D. D. C.; Lidzey, D. G. *J. Appl. Phys.* **1997**, *82*, 6326.
- (11) Wu, C.; Liu, T.-L.; Hung, W.-Y.; Liu, Y.-T.; Wang, K.-T.; Chen, R.-T.; Chen, Y.-M.; Chien, Y.-Y. *J. Am. Chem. Soc.* **2003**, *125*, 3710.

JA0553147